Title

Prenatal presentation of multiple anomalies associated with haploinsufficiency for ARID1A

Journal

European Journal of Medical Genetics, 65(2)

ISSN

1769-7212

Authors

Slavotinek, Anne
Lefebvre, Mathilde
Brehin, Anne-Claire
et al.

Publication Date

2022-02-01

DOI

10.1016/j.ejmg.2021.104407

Peer reviewed

Published in final edited form as:

Eur J Med Genet. 2022 February ; 65(2): 104407. doi:10.1016/j.ejmg.2021.104407.

Prenatal presentation of multiple anomalies associated with haploinsufficiency for *ARID1A*

Anne Slavotinek[a,*], **Mathilde Lefebvre**[b], **Anne-Claire Brehin**[c], **Christel Thauvin**[b], **Sophie Patrier**[c], **Teresa N. Sparks**[d], **Mary Norton**[d], **Jingwei Yu**[e], **Eric Huang**[f]

[a] Dept. Pediatrics, University of California San Francisco, San Francisco, CA, 94143, USA

[b] UFR Des Sciences de Santé, INSERM-Université de Bourgogne UMR1231, Génétique des Anomalies du Développement, Dijon, France

[c] Department of Pathology, CHU Rouen, F-76000, Rouen, France

[d] Department of Obstetrics, Gynecology, & Reproductive Sciences, University of California San Francisco, San Francisco, CA, 94143, USA

[e] Dept. Cytogenetics, University of California San Francisco, San Francisco, CA, 94143, USA

[f] Dept. Pathology, University of California San Francisco, San Francisco, CA, 94143, USA

Abstract

The *ARID1A* gene is an infrequent cause of Coffin-Siris syndrome (CSS) and has been associated with severe to profound developmental delays and hypotonia in addition to characteristic craniofacial and digital findings. We present three fetuses and a male neonate with ventriculomegaly/hydrocephalus, absence of the corpus callosum (ACC), cerebellar hypoplasia, retinal dysplasia, lung lobulation defects, renal dysplasia, imperforate or anteriorly placed anus, thymus hypoplasia and a single umbilical artery. Facial anomalies included downslanting palpebral fissures, wide-spaced eyes, low-set and posteriorly rotated ears, a small jaw, widely spaced nipples and hypoplastic nails. All fetuses had heterozygous variants predicting premature protein truncation in *ARID1A* (c.4886dup:p.Val1630Cysfs*18; c.4860dup:p.Pro1621Thrfs*27; and c.175G>T:p.Glu59*) and the baby's microarray demonstrated mosaicism for a deletion at chromosome 1p36.11 (arr[GRCh37] 1p36.11 (26,797,508_27,052,080)×1~2), that contained the first exon of *ARID1A*. Although malformations, in particular ACC, have been described with CSS caused by pathogenic variants in *ARID1A*, prenatal presentations associated with this gene are rare. Retinal dysplasia, lung lobulation defects and absent thymus were novel findings in

* Corresponding author. anne.slavotinek@ucsf.edu (A. Slavotinek).

CRediT authorship contribution statement

Anne Slavotinek: Conceptualization, Formal analysis, Funding acquisition, Writing – original draft, Writing – review & editing. **Mathilde Lefebvre:** Formal analysis, Writing – original draft, Writing – review & editing. **Anne-Claire Brehin:** Formal analysis, Writing – original draft, Writing – review & editing. **Christel Thauvin:** Formal analysis, Writing – original draft, Writing – review & editing. **Sophie Patrier:** Formal analysis, Writing – original draft, Writing – review & editing. **Teresa N. Sparks:** Formal analysis, Writing – original draft, Writing – review & editing. **Mary Norton:** Formal analysis, Funding acquisition, Writing – original draft, Writing – review & editing. **Jingwei Yu:** Formal analysis, Writing – original draft, Writing – review & editing. **Eric Huang:** Formal analysis, Writing – original draft, Writing – review & editing.

Appendix A. Supplementary data

Supplementary data to this article can be found online at https://doi.org/10.1016/j.ejmg.2021.104407.

association with *ARID1A* variants. Studies in cancer have demonstrated that pathogenic *ARID1A* variants hamper nuclear import of the protein and/or affect interaction with the subunits of SWI/SNF complex, resulting in dysregulation of the PI3K/AKT pathway and perturbed *PTEN* and *PIKC3A* signaling. As haploinsufficiency for *PTEN* and *PIKC3A* can be associated with ventriculomegaly/hydrocephalus, aberrant expression of these genes is a putative mechanism for the brain malformations demonstrated in patients with *ARID1A* variants.

Keywords

Coffin-Siris syndrome; *ARID1A* ; Ventriculomegaly; Hydrocephalus; Prenatal phenotype

1. Introduction

Coffin-Siris syndrome (CSS; OMIM 614607) is a relatively frequent and well-characterized syndrome comprising developmental delays (DD) and intellectual disability (ID), distinctive facial anomalies, hirsutism and hypertrichosis despite sparse scalp hair, aplasia or hypoplasia of the distal phalanx and nail of the fifth digits, and congenital malformations (Schrier Vergano et al., 2013). Feeding difficulties with reduced growth, hearing impairment and ocular defects are also typical (Schrier Vergano et al., 2013). CSS is caused by deleterious variants in the genes comprising the SWItch/Sucrose Non-Fermentable (SWI/SNF) complex, including *ARID1A*, *ARID1B*, *SMARCA2*, *SMARCA4*, *SMARCB1* and *SMARCE1* and others (Tsurusaki et al., 2012; Sweeney et al., 2018).

The *ARID1A* gene encodes the AT-Rich Interactive Domain-containing protein 1A (ARID1A/BAF250a; Pagliaroli and Trizzino, 2021). Pathogenic variants in *ARID1A* are relatively infrequently identified in patients diagnosed with CSS and were reported in 4/63 individuals in one cohort of CSS patients (Santen et al., 2013) and 6/182 patients in another group of CSS patients (Sekiguchi et al., 2019). In 18 patients with CSS previously reported to have causative *ARID1A* variants, clinical features have included profound DD with absent speech, agenesis of the corpus callosum (ACC), congenital heart defects, feeding difficulties, bowel obstruction, and respiratory complications warranting tracheostomy, in addition to the characteristic facial and digital findings associated with CSS (Tsurusaki et al., 2012, 2014; Kosho et al., 2013; Santen et al., 2013; Wieczorek et al., 2013; Kosho et al., 2014a, 2014b; Sekiguchi et al., 2019; Miraldi Utz et al., 2020; Lee and Ki, 2021). Survival in CSS associated with *ARID1A* variants has also been compromised and death from hepatoblastoma at two years of age and from cardiac arrhythmia at one year of age has been described (Kosho et al., 2013). Distinguishing features of CSS in association with *ARID1A* variants have been noted to include facial asymmetry, toenail aplasia, hypoplasia or dysplasia, and scoliosis (Boegershausen and Wollnik, 2018).

Pathogenic *ARID1A* variants have typically comprised frameshift or nonsense variants that were predicted to result in haploinsufficiency and that have involved the entire gene without evidence of a specific hotspot or predilection for the BAF250 domain after exon-size standardization (Santen et al., 2013; Sekiguchi et al., 2019; Pagliaroli and Trizzino, 2021; Lee and Ki, 2021). As homozygosity for loss of function variants in *Arid1a*

results in embryonic lethality in the mouse and mosaicism for *ARID1A* variants has been demonstrated in human patients, it has been hypothesized that all pathogenic *ARID1A* variants occur in mosaic form and that the degree of mosaicism influences clinical variation (Santen et al., 2013; Boegershausen and Wollnik, 2018).

To date, almost all of the patients with CSS caused by pathogenic *ARID1A* variants have been ascertained in the postnatal period. One fetus was identified at 18 weeks of gestation and published in an abstract (Bartin et al., 2018). The fetus had severe intrauterine growth retardation (IUGR) with measurements at the second percentile and multiple malformations, including hydrocephalus and macrocephaly, ACC, a left-sided congenital diaphragmatic hernia (CDH) and a ventricular septal defect (Bartin et al., 2018). An autopsy demonstrated coarse facial features and aplasia of the distal phalanx of the fifth fingers in addition to confirming the malformations visualized prenatally. Sequencing analysis reportedly detected a *de novo ARID1A* pathogenic variant, although the abstract did not provide details of the variant identified (Bartin et al., 2018).

Herein we present three fetuses and a male neonate who were noted to have multiple malformations by ultrasound scanning during pregnancy. All fetuses had truncating variants in *ARID1A*, whereas the male baby was found to have mosaicism for a deletion containing part of the *ARID1A* gene at chromosome 1p36.11. One of the cases was previously reported in a larger study that genotyped 95 fetuses with multiple congenital anomalies (Lefebvre et al., 2021). These cases provide support for a prenatal presentation comprising multiple birth defects in association with haploinsufficiency for *ARID1A*.

2. Case reports

Cases were ascertained by Clinical Geneticists and Pathologists at different institutions and through GeneMatcher (Sobreira et al., 2015). For the neonate, human tissues were collected with written, informed consent and institutional review board (IRB) approval for use for diagnostic, scientific, educational, or therapeutic purposes. For the first and second fetuses, written consent for autopsy and genetic testing were obtained. Ethical approval and written consent were obtained for the third fetus under a protocol approved by the Committee for Human Research at the University of California, San Francisco (protocol #17–22504).

The clinical features of the male patient and fetuses in this report are provided in Supplementary Table 1. For the first patient, the 19-year old, G1P0->1 mother was treated with levetiracetam throughout the pregnancy for grand mal seizures that were diagnosed five years prior to conception. The family history was negative for birth defects and consanguinity and both parents were of Hispanic ancestry. An ultrasound scan at 26 weeks of gestation demonstrated a right-sided CDH containing liver with a lung to head ratio (LHR) of 0.87. Cerebral ventriculomegaly, ACC, cystic dilation of the posterior fossa, kyphoscoliosis of the thoracolumbar spine, a hypocoiled umbilical cord and polyhydramnios with an amniotic fluid index of 29 were also noted. A male baby was delivered at 32 weeks of gestation via forceps-assisted vaginal delivery for premature onset of labor. Birthweight was 1600 g (30th centile corrected for gestational age), length was 43 cm (60th centile corrected for gestational age) and occipitofrontal circumference was 29 cm

(40th centile corrected for gestational age). Apgar scores were 1, 2 and 1 at one, five and 10 min respectively and intubation was required. Physical examination revealed downslanting palpebral fissures, an impression of widely-spaced eyes although interpupillary distance was not measured, a flat nasal bridge with an upturned nasal tip, relatively small, low-set and posteriorly rotated ears, micrognathia, widely-spaced nipples and hypoplastic nails in addition to imperforate anus and bilateral cryptorchidism. Postnatal ultrasound scans confirmed a large, right-sided CDH containing liver and bowel, ACC, and mild enlargement of the temporal horns. A tentative diagnosis of syndromic CDH, including the possibility of Fryns syndrome, was made and after discussion, parents opted for comfort care and the baby was deceased at four days of age. An autopsy confirmed a near total absence of the right posterior diaphragm, with a portion of the right lobe of the liver in the right thorax and lung hypoplasia that was greater on the right side, mesocardia, and malrotation of the small intestines. Ventriculomegaly with ACC, imperforate anus, kyphoscoliosis of the thoracolumbar spine, facial anomalies and hypoplastic nails were verified and downturned corners of the mouth, elongated digits and prominent first toes were also noted. Neuropathology demonstrated ventriculomegaly of the inferior and posterior horns of the lateral ventricles and fourth ventricle without obstruction, ACC, and focal hypoplasia that most prominently affected the cerebellum at the midline.

2.1. Fetus 1

This fetus has previously been reported without photographs in Lefebvre et al. (2021). The pregnancy was achieved using in vitro fertilization for a 36-year old woman. The fetus was a male for whom the pregnancy was interrupted at 23 + 5 weeks of gestation because of severe hydrocephalus (Fig. 1). Weight was 510 g (approximately 25th centile), length was 28 cm (approximately 10th centile) and OFC was 21.5 cm (50–75th centile). An autopsy confirmed hydrocephalus and identified ACC, cerebellar hypoplasia, hypoplasia of the olfactory bulbs and defects of neural migration and cerebral white matter. Heterotaxy with abnormal lung lobulation, a common mesentery, single umbilical artery, right renal dysplasia, pelvic left kidney and shortening of the long bones were also observed. Facial features included widely-spaced eyes and a flat nasal bridge, low-set, posteriorly rotated and dysplastic ears, a long philtrum, macrostomia with thickened lips and bilateral fifth finger clinodactyly.

2.2. Fetus 2

The second fetus was conceived by a 34-year old woman and a 32-year old man who had a healthy son. An ultrasound scan revealed bilateral hydrocephalus with ACC, agenesis of the cerebellar vermis, a ventricular septal defect and an aberrant superior vena cava (Fig. 2). The bladder was not able to be visualized. The parents chose to interrupt the pregnancy at 21 weeks of gestation. At autopsy, growth measurements were compatible with 21 weeks of gestation. External examination showed malar hypoplasia, a short nose with anteverted nares and a long philtum with downturned corners of the mouth. The ears were anomalous, low-set and posteriorly rotated. There was a posterior cleft palate. External genitalia were female and the anus was anteriorly placed. The hands had shortened digits with fifth finger clinodactyly and small nails. Internal examination of the chest revealed abnormal pulmonary lobulation with delayed lung maturation. There was a complete atrioventricular canal defect with a large atrial septal defect, and the superior vena cava arose from the coronary sinus.

The thymus was not visualized and there was a single umbilical artery. Dissection of the brain confirmed hydrocephalus, hypoplasia of the cerebellar vermis and ACC with Probst bundles. There was right retinal dysplasia.

2.3. Fetus 3

The third fetus was conceived by a 34 year old woman and 44 year old man. The woman had a history of multiple, early pregnancy losses. At 13 + 1 weeks, the fetus was found to have an enlarged nuchal translucency measuring 3.8 mm in addition to an omphalocele and occipital encephalocele. Fetal sex was difficult to visualize at the early gestation, but karyotype and microarray confirmed the sex to be male. The fetal size on ultrasound lagged five days behind clinical dating. The pregnancy was interrupted at 14 weeks gestation and pathological examination of the fetal parts was not able to be performed. Due to the early gestational age and lack of autopsy, additional information is not available.

3. Materials and methods

For the neonate, a whole genome single nucleotide polymorphism (SNP)-based cytogenomic array was performed on blood using the Illumina Infinium CytoSNP-850K Beadchip with the Genome Reference Consortium Human Build 37 (GRCh37/hg19). The array platform contained over 850,000 SNPs in 15× redundancy throughout the genome with an exon-centric design to target 3262 genes of known relevance in constitutional and cancer applications. The average probe spacing across the whole array was approximately 1.8 kilobases (kb). Copy number variants (CNVs) in the backbone of the genome involving less than 16 contiguous probes were not reported. Therefore, the overall effective resolution across the whole array was approximately 29 kb. Involvement of a minimum of 12 contiguous probes was required to report a CNV in a critical gene/locus. Classification of clinical significance of CNVs was based on the American College of Medical Genetics and Genomics (ACMG) standards and guidelines (Kearney et al., 2011). For the first fetus, array comparative genomic hybridization (CGH) was performed using a 144K array (Agilent). For the second fetus, array CGH was performed using a 180K Sureprint G3 Human CGH microarray (Agilent).

For the first and second fetuses, solo (proband only) whole exome capture and sequencing were performed on genomic DNA from frozen fetal tissues using the Agilent CRE kit according to the manufacturer's recommendations for paired-end, 76 basepair (bp) reads on an Illumina HiSeq 4000 (Integragen society - Evry, France). Reads were aligned to the human genome reference sequence (GRCh37/hg19 build) with the Burrows-Wheeler Aligner (BWA, v.0.6.2), and potential duplicate paired-end reads were marked with Picard v.1.77. The Genome Analysis Toolkit (GATK) v.2.6–4 was used for base quality score recalibration, indel realignment, and variant discovery (both single-nucleotide variants and indels). Variants were annotated with SeattleSeq SNP Annotation. Rare variants were identified by focusing on protein-altering and splice-site changes present at a frequency less than 1% in dbSNP 138 and the NHLBI GO Exome Sequencing Project. Variants were systematically visualized on the Integrative Genomic Viewer before fetal validation and

familial segregation by Sanger sequencing. The sequencing methodology for the third fetus has previously been published (Mendelsohn et al., 2020).

4. Results

For the male infant, high resolution chromosome analysis revealed a normal male karyotype. The SNP array showed mosaicism for a likely pathogenic copy loss within chromosome 1p36.11, arr[GRCh37] 1p36.11(26,797,508_27,052,080)×1~2, of estimated size 0.254 Mb. The deleted region contained *DHDDS*, *HMGN2*, *DPPA2P2*, *RPS6KA1*, *MIR1976*, *RN7SL679P*, and exon 1 of *ARID1A*, although exons 2–4 were located near the deletion breakpoint. The deletion was confirmed using fluorescence *in-situ* hybridization (FISH; Fig. S1) using probe RP11–492M19 (1p36.11, 26,838,809–26,967,150). Of the 200 interphase cells examined, 103 (51.5%) showed a deletion of 1p36.11 and 97 (48.5%) demonstrated a normal signal pattern. This deletion was reported as likely to be pathogenic, although the laboratory hypothesized that mosaicism for loss of one functional copy of *ARID1A* may not lead to the full phenotypic presentation of CSS. Parental studies were not performed.

For all three fetuses, karyotype and microarray were normal. In the first fetus, exome sequencing revealed a heterozygous, single bp duplication in *ARID1A*, c.4860dup:p.Pro1621Thrfs*27 (NM_006015.6). For the second fetus, exome sequencing revealed heterozygosity for the insertion of a single bp in exon 18 of *ARID1A*, c.4886dup:p. Val1630Cysfs*18 (NM_006015.6). Lastly, exome sequencing identified a *de novo*, heterozygous, stop gain variant in *ARID1A*, c.175G>T; p. Glu59* (NM_006015.6) in the third fetus.

5. Discussion

We report a deceased male infant and three fetuses with clinical findings of ventriculomegaly/hydrocephalus (3/4), ACC (3/4), cerebellar hypoplasia (2/4), olfactory bulb hypoplasia (1/4), and occipital encephalocele (1/4). Additional malformations comprised a complete atrioventricular (AV) canal defect (1/4), CDH (1/4), lung lobulation defects (2/4) with delayed lung maturation (1/4), omphalocele (1/4), imperforate or anteriorly placed anus (2/4) and renal dysplasia (1/4). Retinal dysplasia (1/4), cleft palate (1/4), absent thymus (1/4), kyphoscoliosis of the thoracolumbar spine (1/4) and single umbilical artery (2/4) were also observed. Facial anomalies and digital findings were consistent with those described in CSS when examination was possible, including downslanting palpebral fissures, wide-spaced eyes, low-set and posteriorly rotated ears, micrognathia and hypoplastic nails. All three fetuses had truncating variants predicting haploinsufficiency for *ARID1A*, c.4886dup:p.Val1630Cysfs*18, c.4860dup:p. Pro1621Thrfs*27, and c.175G>T:p.Glu59*. The baby's SNP array demonstrated mosaicism for a deletion that contained the first exon of *ARID1A*, arr 1p36.11 (26,797,508–27,052,080)×1~2.

The findings in the baby and the three fetuses overlap with the previously described facial and digital anomalies and malformation spectrum reported in CSS (Supplementary Table 1). Although patients with postnatal ascertainment of *ARID1A* pathogenic variants

have typically manifest DD, ID and hypotonia, seizures and structural brain abnormalities, including abnormalities of the corpus callosum, can occur (Tsurusaki et al., 2012; Kosho et al., 2013; Kosho et al., 2014a). Phenotypic variation and milder presentations have been associated with mosaicism for *ARID1A* variants, including mosaicism for truncating variants (Santen et al., 2013; Wieczorek et al., 2013).

In contrast to the postnatal presentation, prenatal ascertainment of CSS due to *ARID1A* haploinsufficiency has been rare. It is likely that some of the phenotypic features may be more difficult to ascertain early in gestation and that the prenatal phenotypes of *ARID1A* variants is incompletely characterized. However, with the increasing use of exome sequencing in the prenatal period, it is very likely that additional cases will be identified. Bartin et al. (2018) reported a fetus diagnosed with hydrocephalus and macrocephaly, ACC, a left-sided CDH, ventricular septal defect and severe IUGR. An autopsy demonstrated coarse facies, aplasia of the distal phalanx of the fifth finger and confirmed the organ defects. Sequencing analysis reportedly revealed a *de novo*, pathogenic variant in *ARID1A*, but the variant was not provided in the abstract. The authors noted that IUGR was the most frequent sign in CSS described prenatally and that prenatal description of the cardiac malformations or cleft palate as reported in CSS was extremely rare (Bartin et al., 2018). A second patient with left CDH, aortic arch hypoplasia with small, left-sided cardiac structures, a ventricular septal defect and IUGR was diagnosed with a *de novo*, pathogenic variant in the ATrich DNA interacting domain-containing protein 1B (*ARID1B*) gene, c.3096_3100del-CAAAG (p.Lys1033Arg*fs**32; Sweeney et al., 2018), demonstrating that CDH and cardiac malformations can also occur with other SWI/SNF genes and present prior to the onset of developmental delays. Two additional reports of early presentation of the CSS phenotype, but without molecular genetic testing, have included a male with low birthweight and severe kyphoscoliosis who was deceased at 12 days of age (Suzumura et al., 1996) and a female fetus delivered at 32 weeks of gestation because of ultrasound findings of CDH and cerebellar hypoplasia that was found postnatally to have coarse facies with low-set ears, a low posterior hairline, scalp hypotrichosis and hypoplasia of the fingernails (Delvaux et al., 1998). The presentations depicted in this report are also unique because of the retinal dysplasia, lung lobulation defects, aplasia of the thymus, omphalocele, and occipital encephalocele, which we could not find as being reported in other patients with *ARID1A* variants (Tsurusaki et al., 2012, 2014; Kosho et al., 2013; Santen et al., 2013; Wieczorek et al., 2013; Kosho et al., 2014a; Dillon et al., 2018; Sekiguchi et al., 2019; Miraldi Utz et al., 2020; Lee and Ki, 2021). Widespread retinal pigment epithelial dystrophy with pigment deposits in the mid periphery have been attributed to a missense variant in *SMARCA4* (Cappuccio et al., 2019) and was supported by the disorganized retinal structures, abnormal retinal lamination, and disrupted retinal pigmentation observed in *smarca4* null zebrafish (Zhang et al., 2013, 2014), suggesting that perturbations to the SWI/SNF pathway were the cause. We could not find mention of lung or thymus malformations in association with the other CSS genes.

Many of the malformations described in these cases are not unique to *ARID1A* in CSS. Cardiac anomalies (19.5%), cryptorchidism (55.4%), laryngomalacia (19.8%), and renal anomalies (12.6%) are relatively common in CSS caused by *ARID1B* variants (van der Sluijs et al., 2019). Further examples include absence or hypoplasia of the corpus callosum,

a large posterior fossa, hypoplasia of the cerebellum and cerebellar vermis, enlarged fourth ventricle and absence of the septum pellucidum in association with *ARID1B*, *SMARCB1* and *SMARCE1* variants (Filatova et al., 2019) and CDH associated with *SMARCA4* variants (Scott et al., 2021). However, we are unaware of recognition of a prenatal presentation associated with multiple anomalies in association with other SWI/SNF genes. CSS-causing mutations previously identified in *ARID1A* are heterozygous and have a loss-of-function effect, indicating that *ARID1A* is a dosage-sensitive gene (Tsurusaki et al., 2012; Bidart et al., 2017). Duplications that include *ARID1A* have also been associated with ID and microcephaly (Bidart et al., 2017), and a *de novo* duplication at chromosome 1p36.11 that involved *ARID1A* was described in a child diagnosed with Dubowitz syndrome (Bidart et al., 2017; Dyment et al., 2021). However, organ malformations were not described in these reports of *ARID1A* duplications.

Somatic variants in *ARID1A* are frequent in numerous cancers (Takeda et al., 2016) and hotspots for the somatic variants have been linked to the nuclear export signal sequence that resulted in reduced nuclear export of ARID1A, and to interactions between ARID1A and the other SWI/SNF subunits that disturb the stability of the entire protein complex (Guan et al., 2012). *ARID1A* variants involved in carcinogenesis activate the phosphatidylinositol-3-kinase (PI3K)/AKT pathway and tyrosine kinase receptors, with somatic mutation of specific components of signal transduction, including loss of phosphatase and tensin homolog (PTEN) and activation of mutation of phosphatidylinositol-4, 5-bisphosphate 3-kinase, catalytic subunit α (PIK3CA; Takeda et al., 2016). As deleterious variants in *PTEN* cause Lehrmitte-Duclos disease that can present with hydrocephalus (Almubarak et al., 2019) and haploinsufficiency for *PIK3CA* is known to be associated with hydrocephalus in humans and animal models (Roy et al., 2015), it is tempting to hypothesize that this pathway may also be involved in the developmental malformations seen in the prenatal presentations associated with *ARID1A*. However, further case descriptions and functional studies are needed to investigate this possibility.

Supplementary Material

Refer to Web version on PubMed Central for supplementary material.

Acknowledgements

Dr. Sparks was supported by the National Institutes of Health (NIH) [grant 5K12HD001262–18]. Research reported in this publication was supported by the National Human Genome Research Institute of the National Institutes of Health [grant Award Number U01HG009599]. The content is solely the responsibility of the authors and does not necessarily represent the official views of the National Institutes of Health.

References

Almubarak AO, Haq AU, Alzahrani I, Shail EA, 2019 Mar. Lhermitte-duclos disease with cervical arteriovenous fistula. J. Neurol. Surg. Cent. Eur. Neurosurg. 80 (2), 134–137.

Bartin R, Corizzi F, Melle F, Mechler C, Gavard L, Boutaud de la Combe I, Mandelbrot I, Picone O, 2018. Prenatal diagnosis of Coffin Siris syndrome. Ultrasound Obstet. Gynecol. 52 (Suppl. 1), 66–137 p.136. [PubMed: 28600829]

Bidart M, El Atifi M, Miladi S, Rendu J, Satre V, Ray PF, Bosson C, Devillard F, Lehalle D, Malan V, Amiel J, Mencarelli MA, Baldassarri M, Renieri A, Clayton-Smith J, Vieville G, Thevenon

J, Amblard F, Berger F, Jouk PS, Coutton C, 2017 Jun. Microduplication of the ARID1A gene causes intellectual disability with recognizable syndromic features. Genet. Med. 19 (6), 701–710. [PubMed: 27906199]

Bögershausen N, Wollnik B, 2018 Aug 3. Mutational landscapes and phenotypic spectrum of SWI/SNF-related intellectual disability disorders. Front. Mol. Neurosci. 11, 252. [PubMed: 30123105]

Cappuccio G, Brunetti-Pierri R, Torella A, Pinelli M, Castello R, Casari G, Nigro V, Banfi S, Simonelli F, 2019 Jun. TUDP, Brunetti-Pierri N. Retinal dystrophy in an individual carrying a de novo missense variant of SMARCA4. Mol Genet Genomic Med 7 (6), e682. [PubMed: 30973214]

Delvaux V, Moerman P, Fryns JP, 1998. Diaphragmatic hernia in the Coffin-Siris syndrome. Genet. Counsel. 9 (1), 45–50. [PubMed: 9555587]

Dillon OJ, Lunke S, Stark Z, Yeung A, Thorne N, 2018. Melbourne Genomics Health Alliance, et al. Exome sequencing has higher diagnostic yield compared to simulated disease-specific panels in children with suspected monogenic disorders. Eur. J. Hum. Genet. 26, 644–651. [PubMed: 29453417]

Dyment DA, O'Donnell-Luria A, Agrawal PB, Coban Akdemir Z, Aleck KA, Antaki D, Al Sharhan H, Au PB, Aydin H, Beggs AH, Bilguvar K, Boerwinkle E, Brand H, Brownstein CA, Buyske S, Chodirker B, Choi J, Chudley AE, Clericuzio CL, Cox GF, Curry C, de Boer E, de Vries BBA, Dunn K, Dutmer CM, England EM, Fahrner JA, Geckinli BB, Genetti CA, Gezdirici A, Gibson WT, Gleeson JG, Greenberg CR, Hall A, Hamosh A, Hartley T, Jhangiani SN, Karaca E, Kernohan K, Lauzon JL, Lewis MES, Lowry RB, López-Giráldez F, Matise TC, McEvoy-Venneri J, McInnes B, Mhanni A, Garcia Minaur S, Moilanen J, Nguyen A, Nowaczyk MJM, Posey JE, Õunap K, Pehlivan D, Pajusalu S, Penney LS, Poterba T, Prontera P, Doriqui MJR, Sawyer SL, Sobreira N, Stanley V, Torun D, Wargowski D, Witmer PD, Wong I, Xing J, Zaki MS, Zhang Y,, Care4Rare Consortium, Centers for Mendelian Genomics, Boycott KM, Bamshad MJ, Nickerson DA, Blue EE, Innes AM, 2021 Jan. Alternative genomic diagnoses for individuals with a clinical diagnosis of Dubowitz syndrome. Am. J. Med. Genet. 185 (1), 119–133. [PubMed: 33098347]

Filatova A, Rey LK, Lechler MB, Schaper J, Hempel M, Posmyk R, Szczaluba K, Santen GWE, Wieczorek D, Nuber UA, 2019 Jul 4. Mutations in SMARCB1 and in other Coffin-Siris syndrome genes lead to various brain midline defects. Nat. Commun. 10 (1), 2966. [PubMed: 31273213]

Guan B, Gao M, Wu CH, Wang TL, Shih IeM, 2012 Oct. Functional analysis of inframe indel ARID1A mutations reveals new regulatory mechanisms of its tumor suppressor functions. Neoplasia 14 (10), 986–993. [PubMed: 23097632]

Kearney HM, Thorland EC, Brown KK, Quintero-Rivera F, South ST, 2011 Jul. Working group of the American College of medical genetics laboratory quality assurance committee. American College of medical genetics standards and guidelines for interpretation and reporting of postnatal constitutional copy number variants. Genet. Med. 13 (7), 680–685. [PubMed: 21681106]

Kosho T, Okamoto N, Ohashi H, Tsurusaki Y, Imai Y, Hibi-Ko Y, Kawame H, Homma T, Tanabe S, Kato M, Hiraki Y, Yamagata T, Yano S, Sakazume S, Ishii T, Nagai T, Ohta T, Niikawa N, Mizuno S, Kaname T, Naritomi K, Narumi Y, Wakui K, Fukushima Y, Miyatake S, Mizuguchi T, Saitsu H, Miyake N, Matsumoto N, 2013 Jun. Clinical correlations of mutations affecting six components of the SWI/SNF complex: detailed description of 21 patients and a review of the literature. Am. J. Med. Genet. 161A (6), 1221–1237. [PubMed: 23637025]

Kosho T, Okamoto N, Coffin-Siris Syndrome International Collaborators, 2014a. Genotype-phenotype correlation of Coffin-Siris syndrome caused by mutations in SMARCB1, SMARCA4, SMARCE1, and ARID1A. Am J Med Genet C Semin Med Genet 166C (3), 262–275. [PubMed: 25168959]

Kosho T, Miyake N, Carey JC, 2014b. Coffin-Siris syndrome and related disorders involving components of the BAF (mSWI/SNF) complex: historical review and recent advances using next generation sequencing. Am J Med Genet C Semin Med Genet 166C (3), 241–251. [PubMed: 25169878]

Lee CG, Ki CS, 2021 May 1. A novel *de novo* heterozygous *ARID1A* missense variant cluster in *cis* c.[5954C>G;6314C>T;6334C>T;6843G>C] causes a Coffin-Siris syndrome. Ann Lab Med 41 (3), 350–353. [PubMed: 33303725]

Lefebvre M, Bruel AL, Tisserant E, Bourgon N, Duffourd Y, Collardeau-Frachon S, Attie-Bitach T, Kuentz P, Assoum M, Schaefer E, El Chehadeh S, Antal MC, Kremer V, Girard-Lemaitre F, Mandel JL, Lehalle D, Nambot S, Jean-Marçais N, Houcinat N, Moutton S, Marle N, Lambert

L, Jonveaux P, Foliguet B, Mazutti JP, Gaillard D, Alanio E, Poirisier C, Lebre AS, Aubert-Lenoir M, Arbez-Gindre F, Odent S, Quélin C, Loget P, Fradin M, Willems M, Bigi N, Perez MJ, Blesson S, Francannet C, Beaufrere AM, Patrier-Sallebert S, Guerrot AM, Goldenberg A, Brehin AC, Lespinasse J, Touraine R, Capri Y, Saint-Frison MH, Laurent N, Philippe C, Tran Mau-Them F, Thevenon J, Faivre L, Thauvin-Robinet C, Vitobello A, 2021. Genotype-first in a cohort of 95 fetuses with multiple congenital abnormalities: when exome sequencing reveals unexpected fetal phenotype-genotype correlations. J. Med. Genet. 58 (6), 400–413. 10.1136/jmedgenet-2020-106867. [PubMed: 32732226]

Mendelsohn BA, Beleford DT, Abu-El-Haija A, Alsaleh NS, Rahbeeni Z, Martin PM, Rego S, Huang A, Capodanno G, Shieh JT, Van Ziffle J, Risch N, Alkuraya FS, Slavotinek AM, 2020. A novel truncating variant in ring finger protein 113A (RNF113A) confirms the association of this gene with X-linked trichothiodystrophy. Am. J. Med. Genet. 182, 513–520. [PubMed: 31880405]

Miraldi Utz V, Brightman DS, Sandoval MA, Hufnagel RB, Saal HM, 2020 Sep. Systemic and ocular manifestations of a patient with mosaic ARID1A-associated Coffin-Siris syndrome and review of select mosaic conditions with ophthalmic manifestations. Am J Med Genet C Semin Med Genet 184 (3), 644–655. 10.1002/ajmg.c.31839. [PubMed: 32888375]

Pagliaroli L, Trizzino M, 2021 Mar 4. The evolutionary conserved SWI/SNF subunits ARID1A and ARID1B are key modulators of pluripotency and cell-fate determination. Front. Cell Dev. Biol. 9, 643361. [PubMed: 33748136]

Roy A, Skibo J, Kalume F, Ni J, Rankin S, Lu Y, Dobyns WB, Mills GB, Zhao JJ, Baker SJ, Millen KJ, 2015 Dec 3. Mouse models of human PIK3CA-related brain overgrowth have acutely treatable epilepsy. Elife 4, e12703. 10.7554/eLife.12703. [PubMed: 26633882]

Santen GW, Aten E, Vulto-van Silfhout AT, Pottinger C, van Bon BW, van Minderhout IJ, Snowdowne R, van der Lans CA, Boogaard M, Linssen MM, Vijfhuizen L, van der Wielen MJ, Vollebregt MJ,, Coffin-Siris consortium, Breuning MH, Kriek M, van Haeringen A, den Dunnen JT, Hoischen A, Clayton-Smith J, de Vries BB, Hennekam RC, van Belzen MJ, 2013 Nov. Coffin-Siris syndrome and the BAF complex: genotype-phenotype study in 63 patients. Hum. Mutat. 34 (11), 1519–1528. [PubMed: 23929686]

Schrier Vergano S, Santen G, Wieczorek D, Wollnik B, Matsumoto N, Deardorff MA, 2013 Apr 4. Coffin-siris syndrome. In: Adam MP, Ardinger HH, Pagon RA, Wallace SE, Bean LJH, Stephens K, Amemiya A (Eds.), Gene Reviews® [Internet]. University of Washington, Seattle, Seattle (WA), pp. 1993–2020 [updated 2018 Feb 8].

Scott TM, Campbell IM, Hernandez-Garcia A, Lalani SR, Liu P, Shaw CA, Rosenfeld JA, Scott DA, 2021 Jan 18. Clinical exome sequencing data reveal high diagnostic yields for congenital diaphragmatic hernia plus (CDH+) and new phenotypic expansions involving CDH. J. Med. Genet. 10.1136/jmedgenet-2020-107317 jmedgenet-2020, 107317, Epub ahead of print.

Sekiguchi Tsurusaki Y., Okamoto N, Teik KW, Mizuno S, Suzumura H, Isidor B, Ong WP, Haniffa M, White SM, Matsuo M, Saito K, Phadke S, Kosho T, Yap P, Goyal M, Clarke LA, Sachdev R, McGillivray G, Leventer RJ, Patel C, Yamagata T, Osaka H, Hisaeda Y, Ohashi H, Shimizu K, Nagasaki, K, Hamada J, Dateki S, Sato T, Chinen Y, Awaya T, Kato T, Iwanaga K, Kawai M, Matsuoka T, Shimoji Y, Tan TY, Kapoor S, Gregersen N, Rossi M, Marie-Laure M, McGregor L, Oishi K, Mehta L, Gillies G, Lockhart PJ, Pope K, Shukla A, Girisha KM, Abdel-Salam GMH, Mowat D, Coman D, Kim OH, Cordier MP, Gibson K, Milunsky J, Liebelt J, Cox H, El Chehadeh S, Toutain A, Saida K, Aoi H, Minase G, Tsuchida N, Iwama K, Uchiyama Y, Suzuki T, Hamanaka K, Azuma Y, Fujita A, Imagawa E, Koshimizu E, Takata A, Mitsuhashi S, Miyatake S, Mizuguchi T, Miyake N, Matsumoto N, 2019 Dec. Genetic abnormalities in a large cohort of Coffin-Siris syndrome patients. J. Hum. Genet. 64 (12), 1173–1186. [PubMed: 31530938]

Sobreira N, Schiettecatte F, Valle D, Hamosh A, 2015 Oct. GeneMatcher: a matching tool for connecting investigators with an interest in the same gene. Hum. Mutat. 36 (10), 928–930. [PubMed: 26220891]

Suzumura H, Sakurai K, Kano K, Ichimura T, 1996 Oct. Coffin-Siris syndrome: a case of an extremely low birthweight infant with severe kyphoscoliosis. Acta Paediatr. Jpn. 38 (5), 537–540. [PubMed: 8942018]

Sweeney NM, Nahas SA, Chowdhury S, Campo MD, Jones MC, Dimmock DP, Kingsmore SF, Investigators RCIGM, 2018 Jun 1. The case for early use of rapid whole-genome sequencing in

management of critically ill infants: late diagnosis of Coffin-Siris syndrome in an infant with left congenital diaphragmatic hernia, congenital heart disease, and recurrent infections. Cold Spring Harb Mol Case Stud 4 (3), a002469. [PubMed: 29549119]

Takeda T, Banno K, Okawa R, Yanokura M, Iijima M, Irie-Kunitomi H, Nakamura K, Iida M, Adachi M, Umene K, Nogami Y, Masuda K, Kobayashi Y, Tominaga E, Aoki D, 2016 Feb. ARID1A gene mutation in ovarian and endometrial cancers (Review). Oncol. Rep. 35 (2), 607–613. [PubMed: 26572704]

Tsurusaki Y, Okamoto N, Ohashi H, Kosho T, Imai Y, Hibi-Ko Y, Kaname T, Naritomi K, Kawame H, Wakui K, Fukushima Y, Homma T, Kato M, Hiraki Y, Yamagata T, Yano S, Mizuno S, Sakazume S, Ishii T, Nagai T, Shiina M, Ogata K, Ohta T, Niikawa N, Miyatake S, Okada I, Mizuguchi T, Doi H, Saitsu H, Miyake N, Matsumoto N, 2012 Mar 18. Mutations affecting components of the SWI/SNF complex cause Coffin-Siris syndrome. Nat. Genet. 44 (4), 376–378. [PubMed: 22426308]

Tsurusaki Y, Okamoto N, Ohashi H, Mizuno S, Matsumoto N, Makita Y, Fukuda M, Isidor B, Perrier J, Aggarwal S, Dalal AB, Al-Kindy A, Liebelt J, Mowat D, Nakashima M, Saitsu H, Miyake N, Matsumoto N, 2014 Jun. Coffin-Siris syndrome is a SWI/SNF complex disorder. Clin. Genet. 85 (6), 548–554. [PubMed: 23815551]

van der Sluijs PJ, Jansen S, Vergano SA, Adachi-Fukuda M, Alanay Y, AlKindy A, Baban A, Bayat A, Beck-Wödl S, Berry K, Bijlsma EK, Bok LA, Brouwer AFJ, van der Burgt I, Campeau PM, Canham N, Chrzanowska K, Chu YWY, Chung BHY, Dahan K, De Rademaeker M, Destree A, Dudding-Byth T, Earl R, Elcioglu N, Elias ER, Fagerberg C, Gardham A, Gener B, Gerkes EH, Grasshoff U, van Haeringen A, Heitink KR, Herkert JC, den Hollander NS, Horn D, Hunt D, Kant SG, Kato M, Kayserili H, Kersseboom R, Kilic E, Krajewska-Walasek M, Lammers K, Laulund LW, Lederer D, Lees M, López-González V, Maas S, Mancini GMS, Marcelis C, Martinez F, Maystadt I, McGuire M, McKee S, Mehta S, Metcalfe K, Milunsky J, Mizuno S, Moeschler JB, Netzer C, Ockeloen CW, Oehl-Jaschkowitz B, Okamoto N, Olminkhof SNM, Orellana C, Pasquier L, Pottinger C, Riehmer V, Robertson SP, Roifman M, Rooryck C, Ropers FG, Rosello M, Ruivenkamp CAL, Sagiroglu MS, Sallevelt SCEH, Sanchis Calvo A, Simsek-Kiper PO, Soares G, Solaeche L, Sonmez FM, Splitt M, Steenbeek D, Stegmann APA, Stumpel CTRM, Tanabe S, Uctepe E, Utine GE, Veenstra-Knol HE, Venkateswaran S, Vilain C, Vincent-Delorme C, Vulto-van Silfhout AT, Wheeler P, Wilson GN, Wilson LC, Wollnik B, Kosho T, Wieczorek D, Eichler E, Pfundt R, de Vries BBA, Clayton-Smith J, Santen GWE, 2019 Jun. The ARID1B spectrum in 143 patients: from nonsyndromic intellectual disability to Coffin-Siris syndrome. Genet. Med. 21 (6), 1295–1307. 10.1038/s41436-018-0330-z. Epub 2018 Nov 8. Erratumin: Genet Med. 2019 Jan 29. [PubMed: 30349098]

Wieczorek D, Bögershausen N, Beleggia F, Steiner-Haldenstätt S, Pohl E, Li Y, Milz E, Martin M, Thiele H, Altmüller J, Alanay Y, Kayserili H, Klein-Hitpass L, Böhringer S, Wollstein A, Albrecht B, Boduroglu K, Caliebe A, Chrzanowska K, Cogulu O, Cristofoli F, Czeschik JC, Devriendt K, Dotti MT, Elcioglu N, Gener B, Goecke TO, Krajewska-Walasek M, Guillén-Navarro E, Hayek J, Houge G, Kilic E, Simsek-Kiper Pö, López-González V, Kuechler A, Lyonnet S, Mari F, Marozza A, Mathieu Dramard M, Mikat B, Morin G, Morice-Picard F, Ozkinay F, Rauch A, Renieri A, Tinschert S, Utine GE, Vilain C, Vivarelli, R, Zweier C, Nürnberg P, Rahmann S, Vermeesch J, Lüdecke HJ, Zeschnigk M, Wollnik B, 2013 Dec 20. A comprehensive molecular study on Coffin-Siris and Nicolaides-Baraitser syndromes identifies a broad molecular and clinical spectrum converging on altered chromatin remodeling. Hum. Mol. Genet. 22 (25), 5121–5135. 10.1093/hmg/ddt366. [PubMed: 23906836]

Zhang Y, Bonilla S, Chong L, Leung YF, 2013 Jun-Jul. Irx7, a Smarca4-regulated gene for retinal differentiation, regulates other genes controlled by Smarca4 in zebrafish retinas. Gene Expr. Patterns 13 (5–6), 177–182. [PubMed: 23557786]

Zhang L, Ma P, Collery R, Trowbridge S, Zhang M, Zhong W, Leung YF, 2014 Jan 6. Expression profiling of the RPE in zebrafish smarca4 mutant revealed altered signals that potentially affect RPE and retinal differentiation. Mol. Vis. 20, 56–72. [PubMed: 24426776]

Fig. 1.

Photographs of the first fetus with a truncating variant in *ARID1A* at 23 weeks of gestation. Fig. 1A. Frontal view of fetus, showing widely-spaced eyes, a flat nasal bridge, long philtrum and macrostomia with thickened lips.

Fig. 1B. Profile view of fetus, demonstrating low-set, posteriorly rotated and dysplastic ear.

Fig. 1C. View of the base of the brain and ventricles, demonstrating ventriculomegaly and cerebellar hypoplasia. Ventricular distension has been indicated with an asterisk and cerebellar hypoplasia has been indicated with an arrow.

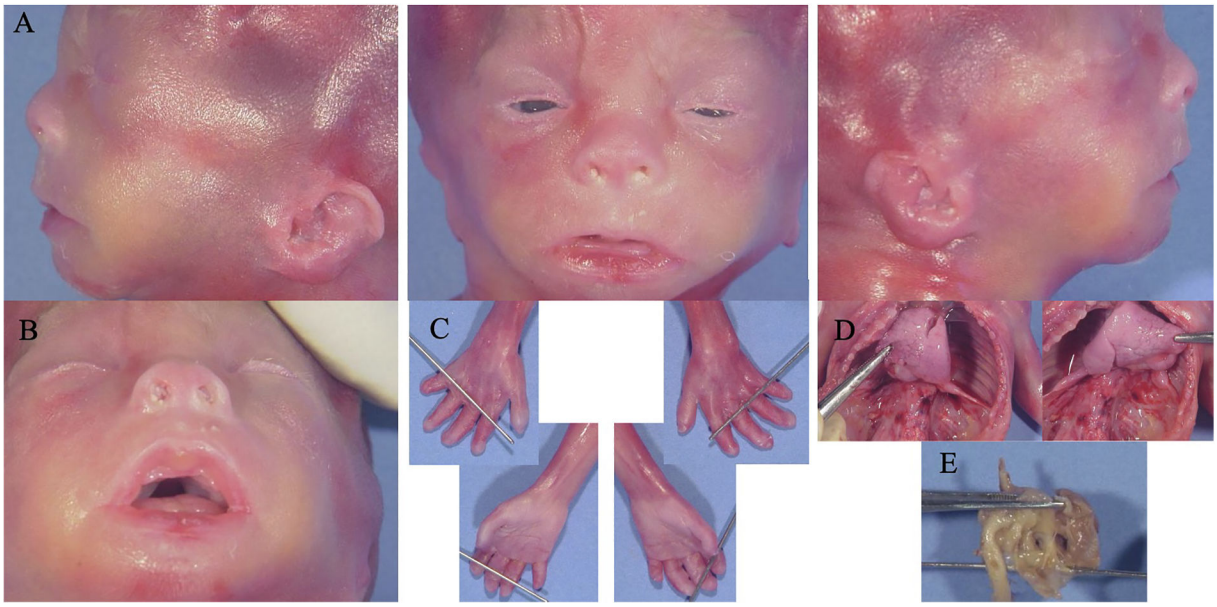

Fig. 2.

Photographs of the second fetus with a truncating variant in *ARID1A* at 21 weeks of gestation.

Fig. 2A. Facial photographs demonstrating midface hypoplasia, a short and anteverted nose, low-set, posteriorly rotated and anomalous ears, and downturned corners of the mouth.

Fig. 2B. Photograph of the mouth, showing cleft palate.

Fig. 2C. Photographs of the hands showing shortened digits with fifth finger clinodactyly and small nails.

Fig. 2D. Photographs of the thoracic cavity, showing pulmonary lobulation defects with delayed lung maturation.

Fig. 2E. Photograph of the heart, showing an atrioventricular canal defect with an ostium primum atrial septal defect and a ventricular septal defect.